Available online at www.sciencedirect.com
SCIENCE DIRECT®
Journal of Solid State Chemistry 177 (2004) 1179–1187
JOURNAL OF SOLID STATE CHEMISTRY
http://elsevier.com/locate/jssc

Synthesis of luminescent bioapatite nanoparticles for utilization as a biological probe

A. Doat,[a] F. Pellé,[b] N. Gardant,[b] and A. Lebugle[a,*]

[a] *CIRIMAT UMR CNRS 5085, Physico-Chimie des Phosphates, ENSIACET-INPT, National Polytechnic Institute of Toulouse, 118 route de Narbonne, 31077 Toulouse, Cedex 4, France*

[b] *Groupe d'Optique des Terres Rares, UMR 7574 Matériaux Inorganiques, 1 place A. Briand, 92195 Meudon, Cedex, France*

Received 23 July 2003; received in revised form 24 October 2003; accepted 26 October 2003

Abstract

A europium-doped apatitic calcium phosphate was synthesized at low temperature (37°C) in water–ethanol medium. This apatite was calcium-deficient, rich in hydrogen phosphate ions, and poorly crystallized with nanometric sized crystallites. It is similar to the mineral part of calcified tissues of living beings and is thus a biomimetic material. The substitution limit of Eu^{3+} for Ca^{2+} ions in this type of bioapatite ranged about 2–3%. The substitution at this temperature was facilitated by vacancies in the calcium-deficient apatite structure. As the luminescence of europium is photostable, the doped apatite could be employed as a biological probe. Internalization of these nanoparticles by human pancreatic cells in culture was observed by luminescence confocal microscopy.

Keywords: Calcium phosphate; Biomimetic apatite; Europium; Luminescence; Biological probe

1. Introduction

Apatites form a large family of compounds with general formula $Me_{10}(XO_4)_6Y_2$ in which *Me* represents a divalent cation (Ca^{2+}, Sr^{2+}, Ba^{2+}), XO_4 a trivalent anion (PO_4^{3-}, VO_4^{3-}, AsO_4^{3-}), and *Y* a monovalent anion (OH^-, F^-, Cl^-). They crystallize in the hexagonal system (space group $P6_3/m$), and their structure is characterized by the existence of tunnels containing mobile *Y* ions. Moreover, many substitutions are possible within this structure, and rare earth ions have been substituted for the Me^{2+} cation [1–9]. However, most of these doped apatites have been synthesized at high temperature (about 1000°C) in a solid-state reaction, or with at least one stage at high temperature. Under such conditions, well-crystallized products are obtained with large crystallites.

For instance, europium-doped silicated oxyapatites (britholites) of general formula Eu: $Ca_{10-x}La_x(SiO_4)_y(PO_4)_{6-y}O_z\square_{2-z}$ fluoridated [1] or unfluoridated [2,3], were synthesized by heating a mixture of powders at 1400°C. In the same way, europium-doped strontium hydroxylapatite, $Sr_{10-x}Eu_x(PO_4)_6O_x(OH)_{2-x}$ [4,5], and europium-doped oxyhydroxylapatite $Ca_{10-x}Eu_x(PO_4)_6O_x(OH)_{2-x}$ [6] have been prepared by heating around 1300°C. Europium-doped borohydroxylapatites have also been synthesized at 1000°C [7], and europium-doped β tricalcium phosphates have been obtained in a solid-state reaction at 1300°C [10–12].

Some syntheses were obtained by precipitation, followed by a high-temperature stage. For example, a europium-doped hydroxylapatite was obtained by precipitation at 100°C, with a subsequent heating at 950°C [8].

Another hydroxylapatite was synthesized by precipitation at 100°C with La^{3+}, and Gd^{3+} ions for luminescence studies [9]. However, the samples were not luminescent, which was assumed to be due to the fact that the ions were only adsorbed on the surface and were not incorporated in the apatitic structure. On the other hand, after heating at 800°C, samples became luminescent as the rare earth ions diffused into the apatitic structure. This accounts for the requirement of a high-temperature stage in the synthesis.

The luminescence of a europium-doped apatite would be of value in biological applications, as unlike the

*Corresponding author. Fax: +33-05-62-88-57-73.
E-mail address: lebugle@cict.fr (A. Lebugle).

0022-4596/$ - see front matter © 2003 Elsevier Inc. All rights reserved.
doi:10.1016/j.jssc.2003.10.023

fluorescent organic molecules usually used as biological probes, the fluorescence of europium is stable with time [13]. Moreover, europium is less sensitive than other rare earths to the decrease in luminescence intensity in the presence of water molecules or high vibration energy groups such as C–H or C–O. These properties point to the interest of a doped apatite as a biological probe. However, as mentioned above, these doped apatites are generally prepared at high temperature. The relatively large crystallites do not interact well with biological media, and they are not readily internalized by living cells. Moreover, in some cases, acicular morphologies are obtained, which can perforate the membranes of cells. By contrast, in living media, the mineral part of bones and teeth is composed of calcium-deficient apatite (containing HPO_4^{2-} ions), with nanometric sized crystallites. It has been shown that such biomimetic apatites can be prepared in a partially aqueous medium [14,15]. The particles obtained are poorly crystallized, which facilitates interactions with cells. We thus examined the possibility of doping a biomimetic calcium-deficient apatite ($Ca_9(PO_4)_5(HPO_4)(OH)$) with europium. The composition and the crystallite sizes of such an apatite should enable it to interact with live cells and therefore be exploited as a biological probe. In order to mix europium ions intimately with the calcium ions, these apatites were synthesized at 37°C by coprecipitating a mixture of Ca^{2+} and Eu^{3+} ions by phosphate ions in water–ethanol medium. We determined the substitution limit of europium in these biomimetic apatites by carrying out the coprecipitation with different percentages of europium. An apatite doped at the substitution limit was then employed as a luminescent probe in a study of its internalization by human pancreatic cells in culture.

2. Materials and methods

2.1. Synthesis

Apatitic tricalcium phosphate was synthesized in hydroalcoholic medium at 37°C under the conditions described by Zahidi et al. and Rodrigues and Lebugle [14,15]. An alcoholic solution containing a calcium salt is rapidly added to another alcoholic solution containing a phosphate salt, with a Ca/P ratio of 1.60. In order to obtain a europium-doped calcium phosphate, europium nitrate was added to the calcium nitrate solution with atomic Eu/(Eu + Ca) ratio ranging 0–20%, and the synthesis was carried out in a similar way. In addition, the compound with Eu/(Eu + Ca) = 100% was also prepared. More specifically, solution A contained a total of 16 mmol of calcium nitrate [$Ca(NO_3)_2 \cdot 4H_2O$] (Carlo Erba) and europium nitrate [$Eu(NO_3)_3 \cdot 6H_2O$] (Alfa Aesar) in the appropriate proportions, dissolved in 33 mL of deionized water and 33 mL of ethanol. Solution B contained 10 mmol of diammonium hydrogen phosphate [$(NH_4)_2HPO_4$] (Prolabo, Normapur) dissolved in 83 mL of deionized water, 15 mL of ammonia (11 M) and 98 mL of ethanol. Solution A was rapidly added to solution B at 37°C while stirring. The precipitate was quickly filtered and washed with a solution containing 60 mL of deionized water, 10 mL of ammonia (11 M) and 70 mL of ethanol. The gel obtained was dried overnight at 70°C.

2.2. Chemical analysis

Europium ion content was determined by induced coupled plasma atomic emission spectroscopy analysis at the Service Central d'Analyse of the CNRS (Vernaison, France) (relative error: 3%). Calcium and europium ions were assayed together by volumetric titration [16] (relative error: 0.5%).

Orthophosphate ions were determined by colorimetry as phosphovanadomolybdenum ($\lambda = 460$ nm) (relative error: 0.5%). The (Ca + Eu)/P atomic ratio had a relative error of 1%.

The residual pyrophosphate ion $P_2O_7^{4-}$ content was determined after calcination of the sample at 600°C for 20 min [17]. This method was used to determine the amount of hydrogen phosphate ions HPO_4^{2-} in the calcium-deficient apatites. Indeed, under these conditions, the maximum condensation of HPO_4^{2-} into $P_2O_7^{4-}$ was attained according to the reaction:

$$2HPO_4^{2-} \rightarrow P_2O_7^{4-} + H_2O.$$

In this case, the $P_2O_7^{4-}$ ions are not able to form the phosphovanadomolybdenum complex and thus could not be assayed by colorimetry. Therefore, the titration gives the residual PO_4^{3-} ions, leading, after subtraction from the total phosphorous content determined above, to the amount of phosphorus atoms as pyrophosphate ions.

However, in some cases, this method is not valid. For example, carbonate and hydrogen phosphate ions present in an apatitic structure react together by heating near 200–300°C according to the reaction:

$$2HPO_4^{2-} + CO_3^{2-} \rightarrow 2PO_4^{3-} + CO_2 + H_2O.$$

The phosphate ion content determined by heating at 600°C is thus underestimated. In a similar way, if HPO_4^{2-} and CO_3^{2-} ions are found in separate phases, they may also react during heating [18,19]. Consequently, the lowering of the initial amount in HPO_4^{2-} ions determined by measuring $P_2O_7^{4-}$ ion content at 600°C can signify the existence of a second phase besides the non-stoichiometric apatite.

2.3. X-ray diffraction (XRD)

XRD patterns were obtained with a CPS 120 INEL diffractometer using the $K\alpha_1$ radiation of a cobalt anticathode. The apparent crystallite size was determined from Scherrer's formula:

$$L_{(hkl)} = \frac{0.94\lambda}{\cos\theta\sqrt{\Delta_r^2 - \Delta_0^2}}$$

with L the apparent size in the direction perpendicular to diffraction plane hkl (Å), 0.94 the Scherrer constant, λ the wavelength of X radiation ($\lambda \mathrm{Co}K\alpha_1 = 1.78892$ Å), θ the diffraction angle corresponding to the considered hkl line, Δ_r the width of the diffraction line of the sample (radian), and Δ_0 the width of the same diffraction line of a well-crystallized hydroxylapatite (radian). It was determined on a hydroxylapatite heated to 900°C.

The (310) and (002) lines were used as suggested by Glimcher [20] to determine the apparent crystallite size in the case of poorly crystallized apatite. The accuracy of the size determined from the (002) line was about 5 Å, whereas the (310) line gave only an estimation of the apparent size.

2.4. FTIR analysis

Infrared spectra within the range 400–4000 cm^{-1} were obtained with a Perkin-Elmer FTIR 1600 spectrometer with pellets comprising 1 mg of powder dispersed in 300 mg of KBr.

2.5. Thermogravimetric analysis (TGA)

TGA was performed in air on about 100 mg of powder with a Setaram Labsys TG apparatus. The temperature was raised from room temperature to 900°C at 3°C/min.

2.6. Transmission electron microscopy (TEM), EDAX, microdiffraction

After dispersion by ultrasound in absolute ethanol, the powder was observed in a JEOL-JEM 2010 electron microscope. Energy dispersion analysis by X-ray (EDAX) and X-ray microdiffraction were also carried out with the same apparatus.

2.7. Luminescence

Luminescence was analyzed through a 1 m monochromator (Jobin–Yvon HR 1000) by a cooled R628 Hamamatsu photomultiplier. The signal was amplified by a 485/4853 Keithley picoammeter. Emission spectra were obtained after excitation at 253.7 nm. Excitation spectra were obtained by monitoring the luminescence at 614 nm (maximal intensity of the emission spectra as described below) and by varying the excitation from 200 to 500 nm. The excitation beam was provided by a 150 W XBO Xenon lamp dispersed by a HD20 Jobin–Yvon monochromator.

3. Results

The calcium, europium and phosphate contents of the powders obtained were determined by chemical analysis. The Eu/(Ca + Eu) and (Ca + Eu)/P atomic ratios are listed in Table 1. It can be seen that the proportion of europium in the powder (Eu/(Ca + Eu) ratio, denoted R_C) is directly related to the ratio Eu/(Ca + Eu) introduced in the liquid (denoted R_L).

Table 1 also indicates that the (Ca + Eu)/P atomic ratio remained close to 1.50 as R_L increased from 0% to 5.55%. This (Ca + Eu)/P value is the same as the Ca/P ratio in tricalcium phosphate. There was a slight increase of this ratio for $R_L > 5.55\%$, i.e., $R_L = 10\%$ and 20%.

The variation with R_C, of the ratio of phosphorus atoms as pyrophosphate ions to the total phosphorus content determined in the samples heated at 600°C, is illustrated in Fig. 1. Up to $R_L = 2\%$, the percentage of P_{pyro} was constant (= 8%). It then fell to near zero.

The compositions of the heated samples deduced from the chemical analyses are listed in Table 2. These formulae were determined by setting the total phosphorus content to one. The OH^- ion content was calculated from electroneutrality.

The X-ray patterns of the 0–10% europium-doped calcium phosphates only exhibited peaks characteristic of a poorly crystallized apatite, with broad lines. The size of the crystallites was calculated from the (002) and (310) lines. For all the samples, they were around 14 nm along the c-axis and 5 nm along the a-axis. The crystallite sizes thus did not depend on R_C. Fig. 2 shows

Table 1
Eu/(Ca + Eu) atomic ratio introduced in the solution (R_L) and determined in the sample (R_C), and (Ca + Eu)/P atomic ratio

Eu/(Ca + Eu) solution (R_L) (atomic %)	Eu/(Ca + Eu) powder (R_C) (atomic %)	(Ca + Eu)/P (atomic)
0	0	1.49
1	1.1	1.50
2	2.1	1.51
3	3.3	1.52
4	4.5	1.52
5.55	5.7	1.52
10	10.1	1.55
20	19.8	1.54
100	100	1.70

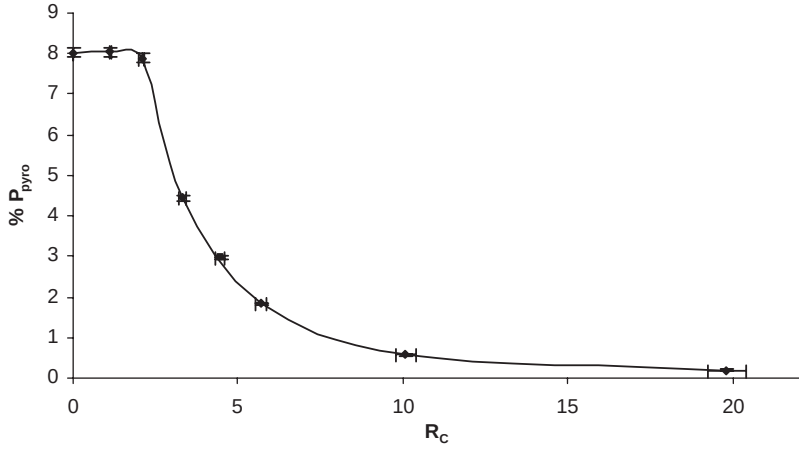

Fig. 1. Plot of phosphorus as pyrophosphate ion content (% P_{pyro}) against R_C in the samples heated at 600°C during 20 min.

Table 2
Composition of the samples heated at 600°C during 20 min. P_{pyro} represents the phosphorus content as pyrophosphate ions

R_L (atomic %)	Composition
0	$Ca_{1.493}Eu_{0.000}(PO_4)_{0.920}(P_{pyro})_{0.080}(OH)_{0.067}$
1	$Ca_{1.487}Eu_{0.017}(PO_4)_{0.920}(P_{pyro})_{0.080}(OH)_{0.103}$
2	$Ca_{1.475}Eu_{0.032}(PO_4)_{0.922}(P_{pyro})_{0.078}(OH)_{0.123}$
3	$Ca_{1.470}Eu_{0.050}(PO_4)_{0.955}(P_{pyro})_{0.045}(OH)_{0.135}$
4	$Ca_{1.452}Eu_{0.068}(PO_4)_{0.970}(P_{pyro})_{0.030}(OH)_{0.138}$
5.55	$Ca_{1.433}Eu_{0.087}(PO_4)_{0.982}(P_{pyro})_{0.018}(OH)_{0.145}$
10	$Ca_{1.392}Eu_{0.157}(PO_4)_{0.993}(P_{pyro})_{0.007}(OH)_{0.260}$
20	$Ca_{1.232}Eu_{0.305}(PO_4)_{0.998}(P_{pyro})_{0.002}(OH)_{0.380}$
100	$Ca_{0.000}Eu_{1.702}(PO_4)_{1.000}(P_{pyro})_{0.000}(OH)_{2.106}$

the X-ray patterns of the samples with $R_L = 0\%$, 2%, and 20%. For $R_L = 20\%$, the presence of a very broad peak in the region of the highest peak is of note, as it is characteristic of a poorly crystalline phase. The XRD pattern of the sample synthesized without calcium ($R_L = 100\%$) indicated that it was a poorly crystallized phase (data not shown), with a very broad peak at 33° (2θ). This value corresponds to the position of the broad peak found for $R_L = 20\%$.

The IR spectra of the compounds with $R_L = 0\%$, 2% and 20% are represented in Fig. 3. Bands characteristic of the phosphate and hydrogen phosphate groups in an apatitic environment were observed: 600, 560 and 1000–1100 cm^{-1} for the PO_4^{3-} groups, and at 875 cm^{-1} for the HPO_4^{2-} ions. Broad bands are characteristic of a poorly crystallized phase. This result is in agreement with the X-ray diffraction patterns, evidencing the poorly crystallized apatitic phase. Moreover, it should be noted that the HPO_4^{2-} band was present in all the spectra, even for high R_L values. The shoulders at 630 and 3560 cm^{-1} stem from OH^- ions. The IR spectra of the samples synthesized with $R_L = 0\%$ to 20% are similar, and the apatitic phase is the only one detected.

The broad band between 670 and 480 cm^{-1} on the samples with $R_C \leqslant 2\%$ was subjected to a computerized mathematical analysis (Grams, Galactica). As described below, samples in this composition range are monophasic. This band was decomposed into one band for apatitic OH^- at 633 cm^{-1}, and other bands for PO_4^{3-} and HPO_4^{2-} groups, as suggested by Bohic and Combes for poorly crystallized apatites [21,22]. The decomposed spectrum of the sample with $R_L = 1\%$ is shown in Fig. 4. The OH^- apatitic band at 633 cm^{-1} and the ratio of its area to the total area of the band between 670 and 480 cm^{-1} were studied in more detail. The plot of this ratio against R_C is shown in Fig. 5, along with the OH^- ion content calculated by electroneutrality. It can be seen that the increases in OH^- ion content with R_C obtained by the two methods were in agreement.

Fig. 6 shows the TGA curve obtained with $R_L = 2\%$. The TGA curves can be divided into two groups:

- For $R_L \leqslant 5.55\%$ two weight loss ranges were observed. The first, between 25°C and 600°C, corresponds to adsorbed water loss and to the condensation of HPO_4^{2-} into $P_2O_7^{4-}$ ions. The second, between 700°C and 850°C corresponds to the reaction of the $P_2O_7^{4-}$ ions with the OH^- ions of the apatitic structure according to the equation:

  $$P_2O_7^{4-} + 2OH^- \rightarrow 2PO_4^{3-} + H_2O.$$

  The second weight loss allowed the pyrophosphate amount present in the sample at 600°C to be determined. Its variation against R_C is illustrated in Fig. 7. It was constant until $R_L = 2\%$ and then decreased to a value close to zero. The pyrophosphate content deduced from TGA did not differ from that obtained by the chemical analysis (Fig. 1).
- For $R_L > 5.55\%$ only the first weight loss was observed. The second loss does not appear as there are no more $P_2O_7^{4-}$ ions at 600°C, as observed by chemical analysis.

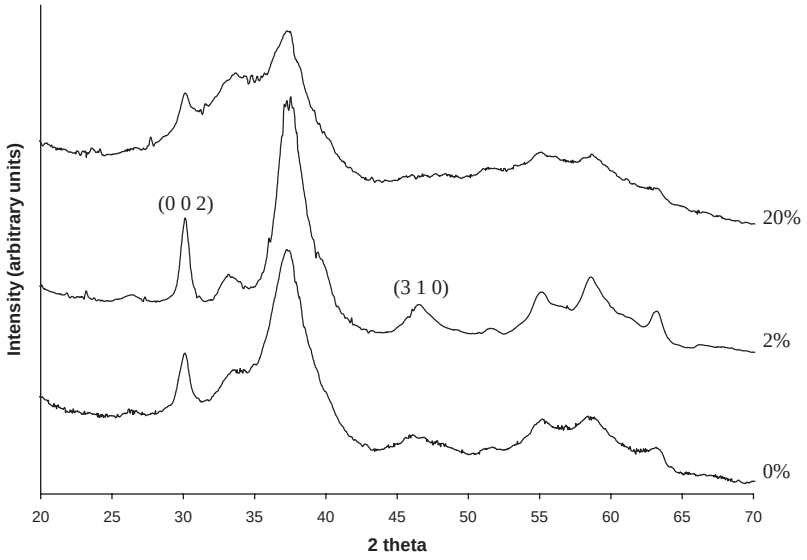

Fig. 2. XRD patterns of the samples synthesized with $R_L = 0\%$, 2% and 20%.

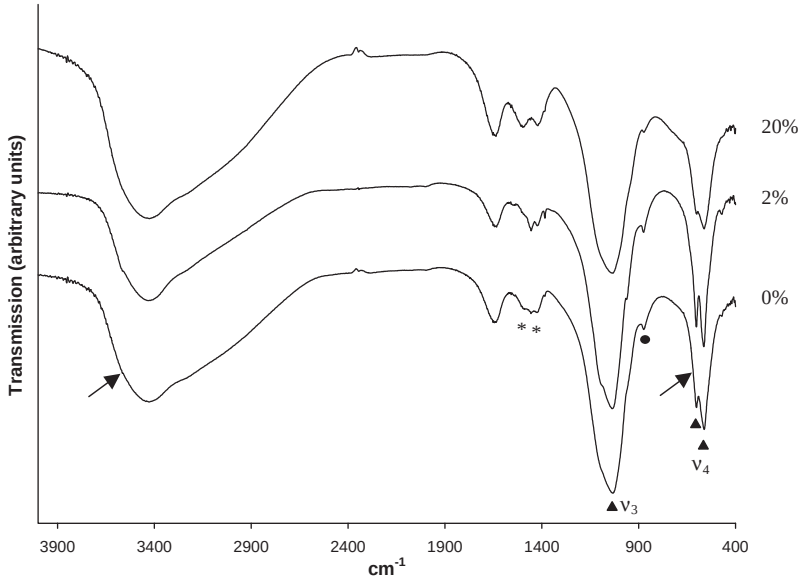

Fig. 3. Transmittance infrared spectra of the samples synthesized with $R_L = 0\%$, 2% and 20%. (▲) PO_4^{3-} regions; (●) HPO_4^{2-} region; (→) OH^- regions; and (*) CO_3^{2-} regions.

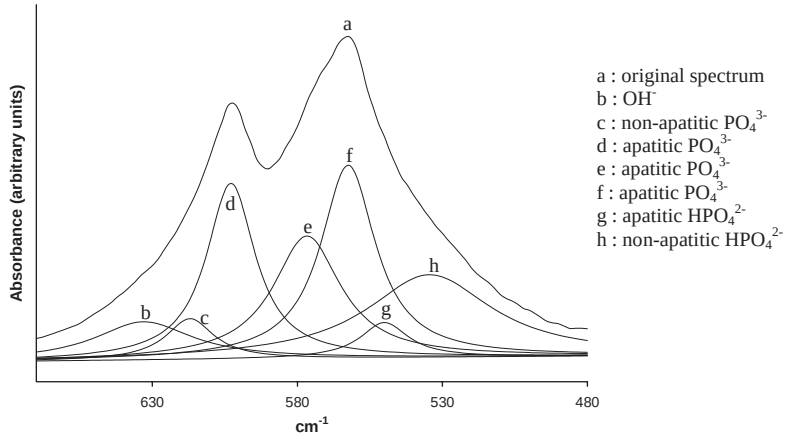

Fig. 4. Decomposition of the IR spectrum between 670 and 480 cm^{-1} for the apatite with $R_C = 1\%$.

We performed TEM observations coupled with EDAX microanalysis on the 2%, 3% and 5.55% europium-doped apatite. The sample with $R_L = 2\%$ was homogeneous and the EDAX measurements indicated a Eu/(Ca + Eu) atomic ratio of around 2.3% in all samples. The (Ca + Eu)/P atomic ratio was around 1.5. These values, within the limits of the accuracy of this analytical method, are in agreement with the chemical analysis. Microdiffraction also confirmed the poorly crystallized apatitic structure of the powder: the rings corresponding to its Miller indices are observed. In contrast, samples with $R_L = 3\%$ and 5% were not homogeneous: the main phase of the sample had an Eu/(Ca + Eu) atomic ratio close to 2%, with a (Ca + Eu)/P atomic ratio close to 1.5, while some localized points were seen to have a very high europium content. Moreover, microdiffraction of this europium-rich phase indicated that it was nearly amorphous. As expected, the presence of this europium-rich phase increased with increase in R_C ratio.

The emission spectrum excited at 253.7 nm obtained on the sample with $R_L = 2\%$ is shown in Fig. 8. Spectral features are observed in three different ranges: 570–582, 582–603 and 603–640 nm. They were ascribed to the $^5D_0 \rightarrow {}^7F_0$, $^5D_0 \rightarrow {}^7F_1$, and $^5D_0 \rightarrow {}^7F_2$ transitions, respectively.

The $^5D_0 \rightarrow {}^7F_0$ domain of the emission spectra was studied in more detail as it may provide more information on the crystallographic sites of europium. A difference was observed between the sample synthesized with $R_L = 2\%$, and the samples with $R_L = 5.55$ and 10% (Fig. 9). Indeed, only one broad peak (579 nm) was observed for $R_L = 2\%$, whereas an additional peak at 577 nm was seen in the samples with $R_L = 5.55$ and 10%. The $^5D_0 \rightarrow {}^7F_0$ transition observed at 579 nm is related to Eu^{3+} ions distributed on Ca^{2+} sites of the

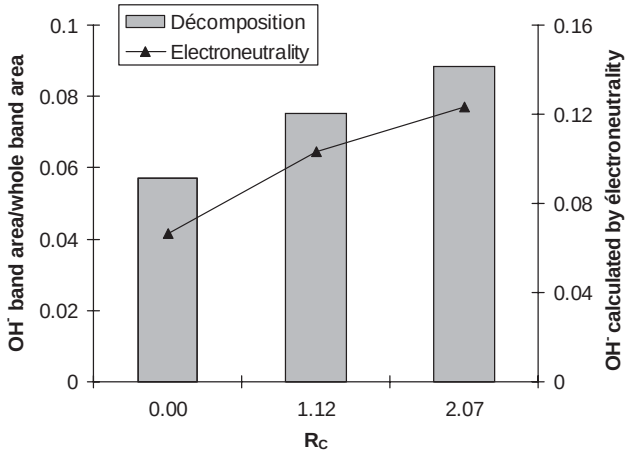

Fig. 5. Plot of the OH^- content of the samples against R_C, obtained by IR spectral analysis and by electroneutrality.

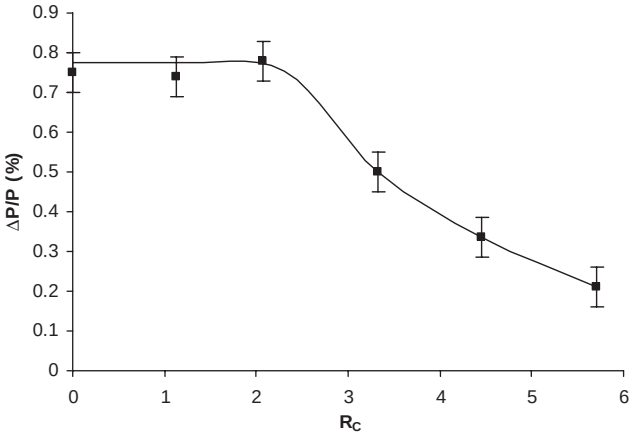

Fig. 7. Variation of the second weight loss (between 700°C and 850°C) against R_C.

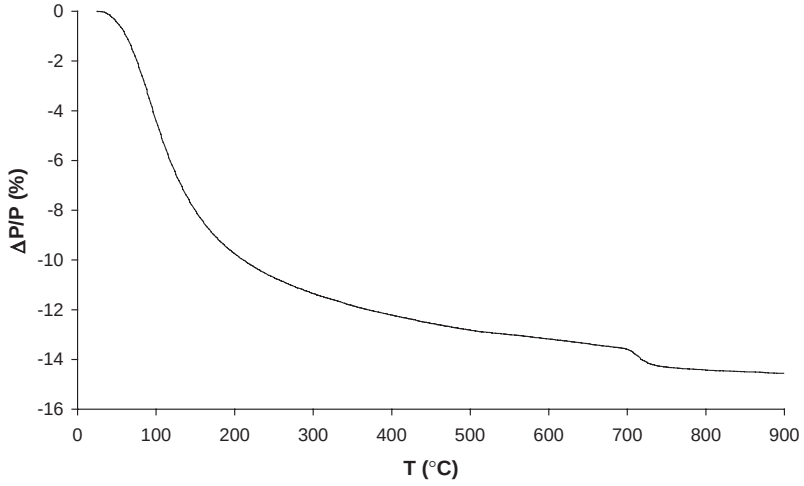

Fig. 6. TGA curve of the apatite synthesized with $R_L = 2\%$ (the weight loss is given with respect to the final weight).

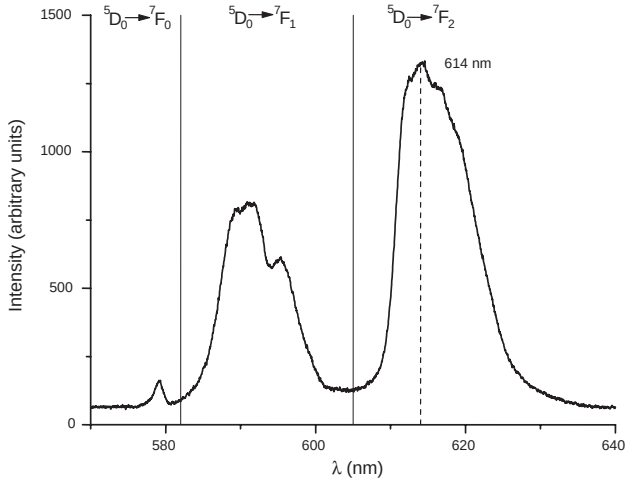

Fig. 8. Luminescence emission spectrum of apatitic tricalcium phosphate with $R_L = 2\%$ (excitation: $\lambda = 253.7$ nm).

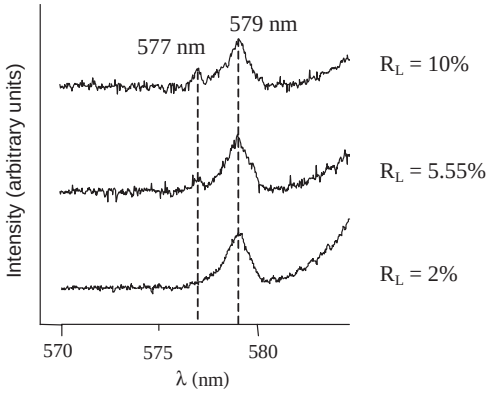

Fig. 9. Details of the $^5D_0 \rightarrow ^7F_0$ transition of the luminescence emission spectra of apatitic tricalcium phosphate with $R_L = 2\%$, 5.55% and 10% (excitation: $\lambda = 253.7$ nm).

apatitic structure. In this case, the nature of the sites for europium ions in this structure, i.e., Ca(I) with C_3 symmetry or Ca(II) with C_s symmetry, cannot be defined due to the poor crystalline state of the material. The second peak which appears at 577 nm with increasing concentration is assigned to Eu^{3+} ions substituted in the minor amorphous phase detected by XRD and TEM analysis of the samples. The more efficient emission was observed for the hypersensitive $^5D_0 \rightarrow ^7F_2$ transition whose maximum intensity was obtained at 614 nm. Therefore, the excitation spectrum was obtained by monitoring the luminescence at 614 nm (Fig. 10). It should be noted that an excitation in the visible domain is possible.

4. Discussion

Studies carried out on europium-doped calcium phosphate have shown that Eu^{3+} ions can substitute

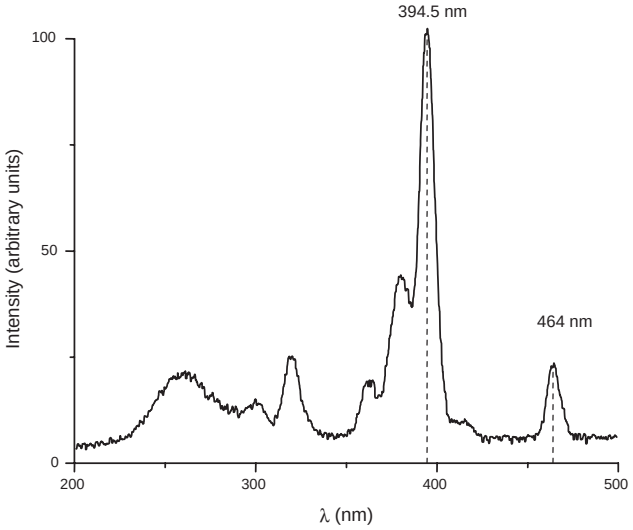

Fig. 10. Luminescence excitation spectrum of apatitic tricalcium phosphate with $R_L = 2\%$ (analysis: $\lambda = 614$ nm).

Table 3
Formulae of the monophasic europium-doped apatitic tricalcium phosphates

R_L (atomic %)	Formula
0	$Ca_{8.96}Eu_{0.00}(PO_4)_{5.52}(HPO_4)_{0.48}(OH)_{0.40}$
1	$Ca_{8.92}Eu_{0.10}(PO_4)_{5.52}(HPO_4)_{0.48}(OH)_{0.62}$
2	$Ca_{8.85}Eu_{0.19}(PO_4)_{5.53}(HPO_4)_{0.47}(OH)_{0.74}$

for Ca^{2+} ions. Indeed, these two ions have similar ionic radii: 0.947 and 1.00 Å, respectively. However, to date the syntheses have been conducted at high temperature.

The use of a water–ethanol medium enabled coprecipitation at 37°C of a poorly crystallized doped apatitic tricalcium phosphate, as shown by chemical analysis, XRD, infrared spectroscopy and luminescence spectra. The analytical results indicated that the samples were monophasic up to a limit between $R_L = 2\%$ and 3%. The Eu^{3+} ions were thus incorporated in the place of Ca^{2+} ions in the apatitic structure.

TEM associated with EDAX showed that the samples were monophasic for $R_L \leqslant 2\%$. This result confirms those of the chemical analysis and TGA, which indicate a change in composition (fall in the condensed phosphate content of the calcined samples, Figs. 1 and 7) above this percentage of europium.

Taken together, these observations suggest that the formulae of the monophasic compounds (Table 3) can be ascribed with a $(PO_4^{3-} + HPO_4^{2-})$ content of 6, which corresponds to the number of groups in the apatitic structure.

Several mechanisms have been proposed to explain the substitution of Eu^{3+} for Ca^{2+} ions in calcium phosphate. In some cases, the substitution of a trivalent ion for a divalent ion is compensated in charge by the

replacement of monovalent OH^- ions by divalent O^{2-} ions in the apatitic structure [4–6,8]. However, this mechanism occurs only at high temperature (about 1000°C), and was not applicable in our case.

A coupled substitution Ca^{2+}, $PO_4^{3-} \leftrightarrow Ln^{3+}$, SiO_4^{4-} has been proposed by other authors to explain the replacement of calcium by a rare earth Ln^{3+} in apatites [1–3]. In another kind of substitution, calcium ions are replaced by monovalent cations M^+ (Na^+) and rare earth ions (case of β tricalcium phosphate in the presence of sodium ions) ($9Ca^{2+} + \square \leftrightarrow 6M^+ + 4Eu^{3+}$) [11]. Such processes could not occur in our experimental conditions (absence of Na^+ or SiO_4^{4-} ions).

The substitution with a vacancy creation ($3Ca^{2+} \leftrightarrow 2Eu^{3+} + \square$) has also been proposed for β tricalcium phosphate [10] and borohydroxylapatites [7]. In our case, this mechanism would lead to a decrease in the (Ca + Eu)/P ratio (it would decrease to 1.48 for $R_L = 2\%$). However, a ratio of 1.51 for the compound with $R_L = 2\%$ was found by chemical analysis. As this is significantly different from the calculated value this mechanism was ruled out.

A coupled substitution involving the replacement of a HPO_4^{2-} ion by a PO_4^{3-} ion may also be envisaged ($Ca^{2+} + HPO_4^{2-} \leftrightarrow Eu^{3+} + PO_4^{3-}$). The substitution of 2% calcium atoms would lead to a decrease of 0.19 in the number of HPO_4^{2-} ions per apatitic lattice. We have seen that the number of HPO_4^{2-} groups per lattice is constant and equal to 0.48 until $R_L = 2\%$, a value significantly different from the one calculated from this mechanism, which was therefore ruled out.

The presence of many anionic vacancies in the tunnels of the tricalcium phosphate might favor the mechanism: $Ca^{2+} + \square \leftrightarrow Eu^{3+} + OH^-$. This would lead to an increase in OH^- ion content of the lattice. It can be seen from Table 3 that the OH^- content increased significantly from 0.40 to 0.74 with increases in R_C from 0% to 2%. We thus concluded that the substitution occurred by this mechanism and that its limit was fixed by the maximal number of OH^- ions which could be introduced in the tunnel of the apatitic tricalcium phosphate crystalline lattice. This is close to the value of 0.8 determined by Rodrigues for undoped apatitic tricalcium phosphate [23]. It should be noted that this maximal OH^- ion content is 0.8 instead of 1 as would be expected from the theoretical formula of the apatitic tricalcium phosphate $Ca_9(PO_4)_5(HPO_4)(OH)$. This compound is formed from amorphous tricalcium phosphate by hydrolysis of PO_4^{3-} ions into HPO_4^{2-} ions according to the reaction:

$$Ca_9(PO_4)_6 + H_2O \rightarrow Ca_9(PO_4)_5(HPO_4)(OH).$$

This lower hydroxyl ion content is due to the high proportion of surface lattices, compared to the core lattices in a nanocrystalline apatite of high specific area as synthesized in hydroalcoholic medium. Rodrigues had interpreted this in terms of a total hydrolysis of a PO_4^{3-} ion in the core lattices, and only partial hydrolysis in surface lattices due to their disrupted structure [15].

Above 3% europium, a europium-rich amorphous phase, detectable by TEM, luminescence, and XRD for $R_L = 20\%$, forms in addition to the limit apatitic phase. This second phase could not be attributed to any known compound. However, we assumed that it corresponded to the compound obtained without calcium ($R_L = 100\%$) that is rich in hydroxide ions of overall chemical formula $Eu_{1.70}(PO_4)(OH)_{2.11}$.

It is of note that above 2% europium, the percentage of phosphorus in the form of pyrophosphate ions after heating the samples to 600°C, decreased rapidly as R_L rose (to 0 at $R_L = 10\%$). This decrease was not due to a decrease in the hydrogen phosphate ion content in the apatitic phase. Indeed, IR showed the continued presence of the HPO_4^{2-} band, even at high percentages of europium. This decrease was attributed to a reaction during heating between the HPO_4^{2-} ions of the apatitic phase and the OH^- ions of the second amorphous phase, which appears from $R_L = 3\%$. Such mechanisms have been demonstrated to occur in intra- or extra-crystalline reactions between HPO_4^{2-} ions and CO_3^{2-} [18,19].

These europium-doped, nanoparticular, calcium-deficient apatites should thus be of value as biological probes. Current biological probes consist of fluorescent organic molecules, which have the disadvantage of undergoing a rapid fall in fluorescence with time (photobleaching) under the effect of the laser excitation. Other mineral photostable probes such as CdSe–CdS or CdSe–ZnS [24,25] are toxic because of cadmium. Europium has a temporally stable luminescence. It can be excited by wavelengths in the visible region and it does not damage cells. Moreover, the apatitic tricalcium phosphate synthesized here is biomimetic and biocompatible. Such compounds would thus make useful luminescent probes as they would allow lengthy observations on living cells. The material synthesized with $R_L = 2\%$ was tested. The sample is monophasic, an essential condition: a high europium content reduces fluorescence yield, and may be cytotoxic. The powdery sample was dispersed in a culture medium in the presence of human cancerous epithelial pancreatic cells (Capan-1 line). After incubation for 30 min, cells were observed by confocal microscopy with laser excitation at 488 nm. Fig. 11 shows the presence of luminescent particles located around the nucleus of the cell. These were doped apatitic tricalcium phosphate particles, which had been internalized by the cell (see Doat [26] for more details). Moreover, it is known that apatites present excellent adsorption properties [27,28]. The nanoparticles of europium-doped bioapatite that we prepared could thus be used after fixation of therapeutic molecules, as luminescent biovectors.

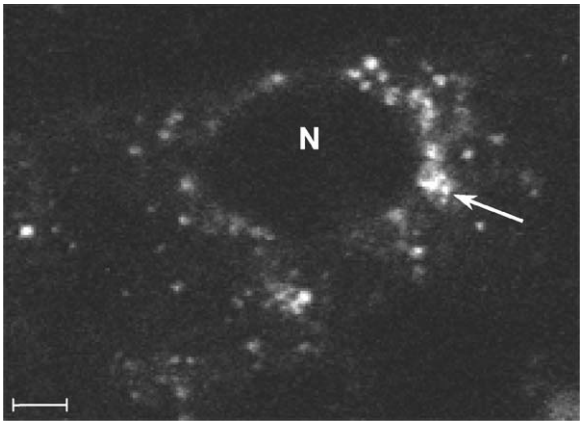

Fig. 11. Visualization of doped calcium phosphate ($R_L = 2\%$) nanoparticles (arrows) internalized in the cytoplasm of human cancerous pancreatic cells in culture observed by confocal laser scanning microscopy. (N) nucleus, (Ap) apical pole. Bar = 1 μm.

5. Conclusion

We synthesized europium-doped apatitic calcium phosphate nanoparticles at low temperature in hydro-alcoholic medium. This rare earth replaced calcium in the apatitic structure up to a proportion of 2–3%. The biocompatibility of this material and the stability of its fluorescence in the visible region confer value as a biological probe. Internalization of these nanoparticles by cells in culture could be readily visualized from their luminescence. Adsorption of organic molecules would enable these apatites to be used as biovectors whose progression in living cells could be monitored from their luminescence.

Acknowledgments

We would like to thank Mr. Datas for the TEM observations and the EDAX and microdiffraction analysis.

References

[1] J. Carpéna, L. Boyer, M. Fialin, J.-R. Kiénast, J.-L. Lacout, C.R. Acad. Sci., Ser. 2, Sci. Terre Planet. 333 (2001) 373–379.
[2] L. Boyer, B. Piriou, J. Carpena, J.-L. Lacout, J. Alloys Compd. 311 (2000) 143–152.
[3] R. El Ouenzerfi, G. Panczer, C. Goutaudier, M.T. Cohen-Adad, G. Boulon, M. Trabelsi-Ayedi, N. Kbir-Ariguib, Opt. Mater. 16 (2001) 301–310.
[4] R. El Ouenzerfi, N. Kbir-Ariguib, M. Trabelsi-Ayedi, B. Piriou, J. Lumin. 85 (1999) 71–77.
[5] J.-L. Lacout, A. Taitai, G. Bonel, C.R. Acad. Sci., Ser. II 304 (13) (1987) 699–702.
[6] A. Taitai, J.-L. Lacout, J. Phys. Chem. Solids 48 (7) (1987) 629–633.
[7] R. Ternane, G. Panczer, M.T. Cohen-Adad, C. Goutaudier, G. Boulon, N. Kbir-Ariguib, M. Trabelsi-Ayedi, Opt. Mater. 16 (2001) 291–300.
[8] R. Ternane, M. Trabelsi-Ayedi, N. Kbir-Ariguib, B. Piriou, J. Lumin. 81 (1999) 165–170.
[9] I. Mayer, J.D. Layani, A. Givan, M. Gaft, P. Blanc, J. Inorg. Biochem. 73 (1999) 221–226.
[10] B.I. Lazoriak, V.N. Golubev, R. Salmon, C. Parent, P. Hagenmuller, Eur. J. Solid State Inorg. Chem. 26 (1989) 455–463.
[11] B.I. Lazoryak, T.V. Strunenkova, V.N. Golubev, E.A. Vovk, L.N. Ivanov, Mater. Res. Bull. 31 (2) (1996) 207–216.
[12] B.I. Lazoryak, T.V. Strunenkova, E.A. Vovk, V.V. Mikhailin, I.N. Shpinkov, A.Y. Romanenko, V.N. Schekoldin, Mater. Res. Bull. 31 (6) (1996) 665–671.
[13] G. Boulon, Actual. Chim. 11 (1999) 96–105.
[14] E. Zahidi, A. Lebugle, G. Bonel, Bull. Soc. Chim. Fr. 4 (1985) 523–527.
[15] A. Rodrigues, A. Lebugle, Colloid Surf. 145 (1998) 191–204.
[16] G. Charlot, Les Méthodes de la chimie analytique, 5th Edition, Masson, Paris, 1966, pp. 658, 853.
[17] A. Gee, V.R. Deitz, J. Am. Chem. Soc. 77 (1955) 2961–2965.
[18] D.J. Greenfield, J.D. Termine, E.D. Eanes, Calcif. Tissue Res. 14 (1974) 131–138.
[19] J.C. Heughebaert, Doctoral Thesis, Toulouse, 1977.
[20] M. Glimcher, L. Bonar, M. Grynpas, W. Landis, A. Roufosse, J. Crystal Growth 53 (1981) 100–119.
[21] S. Bohic, C. Rey, A. Legrand, H. Sfihi, R. Rohanizadeh, C. Martel, A. Barbier, G. Daculsi, Bone 26 (4) (2000) 341–348.
[22] C. Combes, C. Rey, S. Mounic, Key Eng. Mater. 192–195 (2001) 143–146.
[23] A. Rodrigues, Doctoral Thesis, Toulouse, 1998.
[24] M. Bruchez Jr., M. Moronne, P. Gin, S. Weiss, A.P. Alivisatos, Science 281 (1998) 2013–2016.
[25] W.C.W. Chan, S. Nie, Science 281 (1998) 2016–2018.
[26] A. Doat, M. Fanjul, F. Pellé, E. Hollande, A. Lebugle, Biomaterials 24 (2003) 3365–3371.
[27] J.C. Elliot, Structure and Chemistry of the Apatites and Other Calcium Orthophosphates, Vol. 18, Elsevier, Amsterdam, London, New York, Tokyo, 1994, p. 159.
[28] S. Ouizat, A. Barroug, A. Legrouri, C. Rey, Mater. Res. Bull. 34 (14/15) (1999) 2279–2289.